Renner-Teller/Jahn-Teller intersections along the collinear axes of polyatomic molecules: $C_2H_2^+$ as a case study

G. J. Halász
Department of Information Technology, University of Debrecen, P.O. Box 12, H-4010 Debrecen, Hungary

Á. Vibók
Department of Theoretical Physics, University of Debrecen, P.O. Box 5, H-40410 Debrecen, Hungary

D. K. Hoffman
Department of Chemistry and Ames Laboratory, Iowa State University, Ames, Iowa 50011

D. J. Kouri
Department of Chemistry, University of Houston, Houston, Texas 77204-5003 and Department of Mathematics and Physics, University of Houston, Houston, Texas 77204-5003

M. Baer[a)]
The Fritz Haber Research Center for Molecular Dynamics, The Hebrew University of Jerusalem, Jerusalem 91904, Israel

(Received 6 November 2006; accepted 26 February 2007; published online 17 April 2007)

Recently we discussed the Renner-Teller effect in *triatomic* molecules [J. Chem. Phys. **125**, 094102 (2006)]. In that article the main message is that the Renner-Teller phenomenon, just like the Jahn-Teller phenomenon, is a *topological* effect. Now we extend this study to a *tetra-atomic* system, namely, the $C_2H_2^+$ ion, for which topological effects are revealed when one atom surrounds the triatom axis or when two atoms surround (at a time) the *two-atom* axis. The present study not only supports the findings of the previous study, in particular, the crucial role played by the *topological* **D** matrix for diabatization, but it also reveals new features which are expected to be more and more pronounced the larger the original *collinear* molecule. As already implied, shifting away two atoms from the collinear molecular axis does not necessarily abolish the ability of the remaining two atoms to form topological effects. Moreover, the study indicates that when the two hydrogens are shifted away, the CC axis produces *two* kinds of topological effects: (1) a Renner-Teller effect (characterized by a topological phase of 2π) which is revealed when the two hydrogens surround, rigidly, this axis (as mentioned above), and (2) a Jahn-Teller effect (characterized by a topological phase of π) which is revealed when one of the hydrogens surrounds this axis while the other hydrogen is clamped to its position. © *2007 American Institute of Physics*.
[DOI: 10.1063/1.2717934]

I. INTRODUCTION

Recently, while studying triatom molecules, we suggested considering the Renner-Teller (RT) effect as a topological phenomenon caused by degeneracy points located along the collinear axis of the studied molecule.[1] As a first example of such a treatment we chose the NH_2 molecule for which the degeneracy is formed along this axis by the two degenerate Π states $^2B_1$ and $^2A_1$.[1,2] According to the Jahn-Teller (JT) terminology such a line of degeneracy points is called a *seam* and the topological phenomenon is revealed by employing closed contours, Γ, that surround these seams.[3] To be more specific, just like in the study of the JT effect, we calculate the corresponding electronic nonadiabatic coupling terms (NACTs) and follow their behavior (as will be elaborated below) along these *open* and *closed* Γ contours.

The main emphasis in the study of the RT effects is usually on the (adiabatic) potential energy surfaces[4] but issues related to the NACTs are in most cases ignored and therefore difficulties associated with the *diabatization* process are not always properly treated. In order for the diabatization to have a physical meaning the newly constructed diabatic surfaces have to be *single valued* and this can be guaranteed if the orbital (angular) quantum number Λ is an integer (or half an integer). It is well known that Λ is indeed an integer for collinear configurations[4–9] but it deviates from an integer for other configurations.[4,10–17] The main assumption in such instances is that the deviations are not large and can be ignored. Still, efforts were made to partly correct for this mishap.[10–12]

In Ref. 2 we present a different approach to overcome the above mentioned difficulty, an approach which is successfully applied in the case of the JT intersection.[18] It is based on the fact that the RT phenomenon is, in many ways, similar to the JT phenomenon.[18–31] The similarity becomes apparent due to the fact that, like the JT points of degeneracy (that are distributed along infinite long *seams*), the RT points of degeneracy, which are distributed along segments of the collinear molecular axis, also form *infinite* long seams. That

[a)]Electronic mail: michaelb@fh.huji.ac.il

said, the two phenomena still differ to some extent (at least in the case of planar molecules) because the JT intersection is formed by states of the same symmetry whereas the RT intersection is formed by states of different symmetries. Other differences are discussed below.

Whereas the emphasis in our first publication is on the *triatomic* systems[1,2] the present study centers on *tetra-atomic* systems.[4,17] In particular, we show that difficulties in the *diabatization* as encountered for tetra-atomic systems can be remedied in the same way as is done in triatomic systems. However, having four atoms opens up numerous new and interesting possibilities. These are not necessarily related to the diabatization process itself but concern new features formed by the RT intersection.

In 1934 Renner[5] published a detailed study of a linear polyatomic molecule, characterized by an electronic orbital angular momentum component $\Lambda\hbar$ (where $\Lambda \neq 0$) and by an angular momentum component, $\ell\hbar$, associated with the bending vibrations of the molecule, both defined with respect to the original (collinear) molecule axis, considered to be the z axis.[5] To be more specific, in that study Renner concentrated on those states that split to become two (coupled) states when moving away from collinearity. Thus if we consider, e.g., a Π state characterized by the quantum number $\Lambda=1$ and a single eigenfunction, $\zeta_{\Lambda=1}(\mathbf{s}_e|\mathbf{s})$, then, after moving away from collinearity, one encounters two eigenfunctions, namely, $\zeta^{\pm}_{\Lambda=1}(\mathbf{s}_e|\mathbf{s})$ related to the two decoupled states (in this notation $\mathbf{s}_e$ and $\mathbf{s}$ stand for the collective electronic and nuclear coordinates, respectively). We do not intend to elaborate any further on the Renner model (this was done in Ref. 2) but immediately refer to the Born-Oppenheimer (BO) treatment and continue our presentation employing the above mentioned NACTs.[30,31]

The NACT in general is a *vectorial* entity that couples two given electronic adiabatic states so that if $\boldsymbol{\tau}_{jk}(\mathbf{s})$ is the term that couples states j and k then it can be written as[30]

$$\boldsymbol{\tau}_{jk}(\mathbf{s}) = \langle \zeta_j(\mathbf{s}_e|\mathbf{s}) | \nabla \zeta_k(\mathbf{s}_e|\mathbf{s}) \rangle. \tag{1}$$

In what follows we use cylindrical coordinates (q,φ,z) where q and φ are the (planar) polar coordinates (q the radius and φ the angle) and z the coordinate perpendicular to this plane. Of the various possible components of $\boldsymbol{\tau}_{jk}(\mathbf{s})$ the ones of main interest for us is the angular components related to a rotation around the (collinear) molecular axis (which is assumed to be located along the z axis). If φ is the angle associated with this (nuclear) rotation then the corresponding angular component can be written as $(1/q)\boldsymbol{\tau}_{\varphi jk}(\mathbf{s})$, where

$$\boldsymbol{\tau}_{\varphi jk}(\mathbf{s}) = \left\langle \zeta_j(\mathbf{s}_e|\mathbf{s}) \left| \frac{\partial}{\partial \varphi} \zeta_k(\mathbf{s}_e|\mathbf{s}) \right. \right\rangle. \tag{2}$$

Here, $\zeta_i(\mathbf{s}_e|\mathbf{s})$; $i=j,k$ are the electronic eigenfunctions introduced earlier and q is the radial coordinate that together with φ forms the two polar coordinates associated with the rotation in a plane. In other words q is a distance from the collinear axis.

As mentioned earlier, in the present article we consider the collinear tetra-atomic system $C_2H_2^+$ ion[4,17,32] and consequently all details to be mentioned are related to this ion.

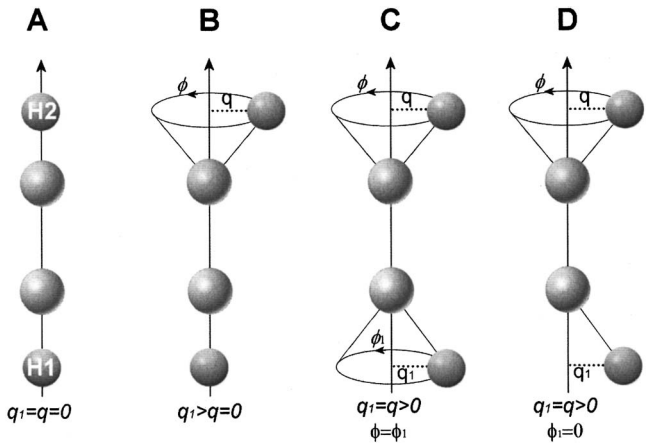

FIG. 1. The various configurations of a tetra-atomic system treated in the article: (A) the collinear tetra-atomic arrangement; (B) the *symmetric* case formed by a single atom surrounding the triatom axis; (C) the *symmetric* case formed by a rigid rotation of two atoms surrounding the C–C axis; (D) the *nonsymmetric* case formed by one shifted (clamped) atom and one atom surrounding the C–C axis.

As mentioned above we assume the four (collinear atoms) to be located along the z axis with the origin being at some point along this axis [see Fig. 1(A)]. Consequently the coordinates of the four (collinear) atoms are $\mathbf{s}=(z_1,z_2,z_3,z_4)$. In all numerical treatments the two carbons are clamped at the molecular axis and only the hydrogens, to be labeled as H1 and H2, may be shifted from the axis. To carry out the calculations of the angular NACT [see Eq. (2)] and later, the line integral, we distinguish between two situations, namely, (a) when one atom, H2, is shifted from the axis and is allowed to surround the molecular axis [see Fig. 1(B)] and (b) when two atoms, H1 and H2, are shifted from the axis and both surround that axis simultaneously [see Fig. 1(C)]. In what follows the position of each of the two hydrogens H1 and H2 is described in terms of cylindrical coordinates. This means that in addition to the z coordinate their position is determined by the (polar) coordinates (q_1,φ_1) and (q_2,φ_2), respectively. From now on we refer to the general coordinate $\mathbf{s}$ as (q,φ) thus ignoring the z coordinates altogether.

Next we mention (briefly) one additional situation that will be studied extensively, namely, the case where both hydrogens, H1 and H2, are shifted away from axis but only one atom, H2, surrounds the (molecular) z axis [see Fig. 1(D)].

II. THEORY

A. Background comments

In Ref. 2 we presented in detail the connection between the JT and RT frameworks while justifying the application of the theory for the RT intersections, originally developed for the JT intersections. This part will not be repeated here but, for the sake of completeness, we just list the main expressions.

Having the BO adiabatic (diagonal) potential matrix, $\mathbf{u}(\mathbf{s})$, the diabatic potential matrix $\mathbf{W}(\mathbf{s})$ is obtained following the adiabatic-to-diabatic transformation (ADT) matrix $\mathbf{A}(\mathbf{s})$,

$$\mathbf{W}(\mathbf{s}) = \mathbf{A}^{\dagger}(\mathbf{s})\mathbf{u}(\mathbf{s})\mathbf{A}(\mathbf{s}). \tag{3}$$

The ADT matrix can be shown to be an orthogonal (unitary) matrix that fulfills the following first order differential (vector) equation:[33]

$$\nabla\mathbf{A}(\mathbf{s}) + \boldsymbol{\tau}(\mathbf{s})\mathbf{A}(\mathbf{s}) = \mathbf{0}, \tag{4}$$

where $\boldsymbol{\tau}(\mathbf{s})$ is the nonadiabatic coupling matrix (NACM) with the elements as defined in Eq. (1). The solution of this equation can be written as an exponentiated line integral,[34]

$$\mathbf{A}(\mathbf{s}|\mathbf{s}_0,\Gamma) = \wp \exp\left(-\int_{\mathbf{s}_0}^{\mathbf{s}} d\mathbf{s}\cdot\boldsymbol{\tau}(\mathbf{s}|\Gamma)\right)\mathbf{A}(\mathbf{s}_0), \tag{5}$$

where $\wp$ is the *ordering* operator, $\mathbf{s}_0$ is the initial point of integration, Γ is the contour along which Eq. (4) is required to be solved, the dot stands for a scalar product, and $\mathbf{A}(\mathbf{s}_0)$ is the initial value of $\mathbf{A}(\mathbf{s})$ on Γ. In what follows $\mathbf{A}(\mathbf{s}_0)$ is assumed to be the *unit* matrix. It is well noticed that the only component of $\boldsymbol{\tau}(\mathbf{s})$ that contributes to the line integral is the *tangential* component along the contour, Γ.

Another matrix of interest is the *topological* matrix $\mathbf{D}(\Gamma)$ which is identical to the $\mathbf{A}$ matrix but is calculated along a *closed* contour,[18]

$$\mathbf{D}(\Gamma) = \mathbf{A}(\mathbf{s}_0|\mathbf{s}_0,\Gamma) = \wp \exp\left(-\oint_{\Gamma} d\mathbf{s}\cdot\boldsymbol{\tau}(\mathbf{s}|\Gamma)\right). \tag{6}$$

The $\mathbf{D}$ matrix does not depend on any specific point along Γ but on the contour as a whole. It can be shown that in order for the diabatic potential matrix $\mathbf{W}(\mathbf{s})$ to be *single valued* in the region of interest, the $\mathbf{D}$ matrix has to be *diagonal* for any chosen closed contour Γ in the region. Since $\mathbf{D}(\Gamma)$ [just like $\mathbf{A}(\mathbf{s})$] is unitary its elements are expected to be[18]

$$\mathbf{D}_{jk}(\Gamma) = \delta_{jk}\exp(i\theta_j(\Gamma)), \quad j=\{1,N\}, \tag{7}$$

where $\theta_j(\Gamma)$; $j=\{1,N\}$ are real phases. In the case of real *eigenfunctions* the phases become integer multiples of π so that the $\mathbf{D}$-matrix elements are

$$\mathbf{D}_{jk}(\Gamma) = \pm\delta_{jk}, \quad j=\{1,N\}. \tag{8}$$

Next we briefly analyze what happens in case Γ is chosen to be a circle defined by the position of its center and the relevant radius q. In this situation the ADT matrix can be written as

$$\mathbf{A}(\varphi|q,\Gamma) = \wp \exp\left(-\int_0^{\varphi} d\varphi\boldsymbol{\tau}_{\varphi}(\varphi|q,\Gamma)\right), \tag{9}$$

where we identify $(1/q)\boldsymbol{\tau}_{\varphi}(\varphi|q)$ as the angular component of $\boldsymbol{\tau}$. In the same way the topological matrix $\mathbf{D}$ takes the form

$$\mathbf{D}(q,\Gamma) = \wp \exp\left(-\int_0^{2\pi} d\varphi\boldsymbol{\tau}_{\varphi}(\varphi|q,\Gamma)\right). \tag{10}$$

Earlier we emphasized the fact that the condition for the diabatic potentials to be single valued is the fulfillment of Eq. (8). Moreover, it is seen that the single valuedness is solely determined by the NACM. Therefore in order to find out if a group of N states is capable of yielding single-valued diabatic potentials all that is necessary is to calculate the corresponding $N\times N$ $\mathbf{D}$ matrix and see to what extent it is diagonal.

In case of two states, Eqs. (9) and (10) simplify significantly because any 2×2 orthogonal matrix can be written in terms of

$$\mathbf{A}^{(2)}(\varphi,q) = \begin{pmatrix} \cos(\gamma_{12}(\varphi,q)) & \sin(\gamma_{12}(\varphi,q)) \\ -\sin(\gamma_{12}(\varphi,q)) & \cos(\gamma_{12}(\varphi,q)) \end{pmatrix}, \tag{11}$$

where $\gamma_{12}(\varphi,q)$ is the ADT angle expressed in terms of a line integral,

$$\gamma_{12}(\varphi,q) = \int_0^{\varphi} \boldsymbol{\tau}_{\varphi 12}(\varphi',q)d\varphi'. \tag{12}$$

A similar expression is given for $\alpha_{12}(q)$, the topological (Berry) phase, namely,

$$\alpha_{12}(q) = \int_0^{2\pi} \boldsymbol{\tau}_{\varphi 12}(\varphi',q)d\varphi'. \tag{13}$$

The corresponding $\mathbf{D}$ matrix is similar to the $\mathbf{A}$ matrix as given in Eq. (11) but where $\alpha_{12}(q)$ replaces $\gamma_{12}(\varphi,q)$, namely,

$$\mathbf{D}^{(2)}(q) = \begin{pmatrix} \cos(\alpha_{12}(q)) & \sin(\alpha_{12}(q)) \\ -\sin(\alpha_{12}(q)) & \cos(\alpha_{12}(q)) \end{pmatrix}. \tag{14}$$

It is well noticed that the condition for the $\mathbf{D}$ matrix to be *diagonal* is that

$$\alpha_{12}(q) = 2\pi n, \tag{15}$$

where n is an integer or half an integer.

Comments. (1) We found that a group of N states yields a single-valued diabatic potential if and only if this group is approximately isolated with respect to the rest of the states that form the complete Hilbert space. This happens when the NACTs of the type $\boldsymbol{\tau}_{jk}$, that couple any state j within the group of N states with any state k outside that group, are negligibly small, i.e., $|\boldsymbol{\tau}_{jk}| \sim \mathrm{O}(\varepsilon)$. In such a case this group of N states forms a Hilbert subspace [more about this issue can be found in Refs. 27(a) and 33(b)]. (2) In what follows we treat only the *angular* component of $\boldsymbol{\tau}$. Consequently we drop the subscript φ so that $\boldsymbol{\tau}$ and $\boldsymbol{\tau}_{jk}$ stand for $\boldsymbol{\tau}_{\varphi}$ and $\boldsymbol{\tau}_{\varphi_{jk}}$, respectively.

B. Treatment of symmetrical NACTs

One of the features that characterize the treatment of the Renner-Teller intersection is that frequently their NACTs can be chosen to be independent of the polar angle, φ. This happens when the *centers* of the circular contours, Γ, are located on the molecular axis. In such a case we find that, due to this symmetry [see Fig. 1(B)], the integration in Eqs. (10) and (13) can be carried out trivially.

In what follows we distinguish between the case where the $\boldsymbol{\tau}$ matrix is of 2×2 dimension and the case where it is of the 3×3 dimension (thus, the first case applies to the two-state Hilbert subspace and the second to the three-state Hilbert subspace).

1. The two-state Hilbert subspace

In this case the $\boldsymbol{\tau}$ matrix is of the form

$$\boldsymbol{\tau}(q)=\begin{pmatrix}0 & 1\\ -1 & 0\end{pmatrix}\tau_{12}(q), \tag{16}$$

and since τ_{12} does not depend on the angle φ the corresponding **D** matrix becomes [see Eq. (14)]

$$\mathbf{D}^{(2)}(q)=\begin{pmatrix}\cos(2\pi\tau_{12}) & \sin(2\pi\tau_{12})\\ -\sin(2\pi\tau_{12}) & \cos(2\pi\tau_{12})\end{pmatrix}. \tag{17}$$

In order for the **D** matrix to be diagonal τ_{12} has to fulfill the condition

$$\tau_{12}(q)=\begin{cases} n & \text{(18a)}\\ (2n+1)/2, & \text{(18b)}\end{cases}$$

where n is an integer. In other words, the two states under consideration form a Hilbert *subspace* in a region defined by q if and only if for each q value in that region n is an integer. It is important to mention that case Eq. (18)(a) applies to the RT intersection and Eq. (18)(b) to a (single) JT intersection.

2. The three-state Hilbert subspace

Here, like in the previous case, the $\boldsymbol{\tau}$-matrix elements do not depend on φ so that the **D** matrix takes the form [see Eq. (10)]

$$\mathbf{D}(q)=\exp(-2\pi\boldsymbol{\tau}(q)). \tag{19}$$

To treat the three-state case we assume the 3×3 $\boldsymbol{\tau}$ matrix to be of the form

$$\boldsymbol{\tau}(q)=\begin{pmatrix}0 & \tau_{12}(q) & 0\\ -\tau_{12}(q) & 0 & \tau_{23}(q)\\ 0 & -\tau_{23}(q) & 0\end{pmatrix}, \tag{20}$$

so that $\tau_{13}(q)$ is assumed to be negligibly small. Next, substituting Eq. (20) in Eq. (19) yields, the following **D** matrix:[18]

$$\mathbf{D}^{(3)}(q)=\omega^{-2}\begin{pmatrix}\tau_{23}^2+\tau_{12}^2C & \tau_{12}\omega S & \tau_{12}\tau_{23}(1-C)\\ \tau_{12}\omega S & \omega^2C & -\tau_{23}\omega S\\ \tau_{12}\tau_{23}(1-C) & \tau_{23}\omega S & \tau_{12}^2+\tau_{23}^2C\end{pmatrix}, \tag{21}$$

where

$$C=\cos(2\pi\omega),\quad S=\sin(2\pi\omega),\quad \omega=\sqrt{\tau_{12}^2+\tau_{23}^2}, \tag{22}$$

and we recall that $\tau_{jk}=\tau_{jk}(q)$. It is well noticed that the $\mathbf{D}^{(3)}$ matrix in Eq. (21) becomes diagonal if and only if $\omega=n$, where n is an integer. It is interesting to mention that the eigenvalues of $\boldsymbol{\tau}(q)$ are $\{i\omega,-i\omega,0\}$ and therefore if $n=1$ we get that the eigenvalues of $\boldsymbol{\tau}(q)$ are $\{i,-i,0\}$.

Since our main concern are the diagonal elements of the $\mathbf{D}^{(3)}$ matrix we calculate them employing the following expressions:

$$(D_{11},D_{22},D_{33})=\left(\frac{\tau_{12}^2C+\tau_{23}^2}{\tau_{12}^2+\tau_{23}^2},C,\frac{\tau_{12}^2+\tau_{23}^2C}{\tau_{12}^2+\tau_{23}^2}\right). \tag{23}$$

It is noticed that for those cases for which ω is an integer all three diagonal elements are equal to 1.

3. Summary

In Sec. II B we analyzed the two-state case and the three-state case. For the two state-case we found that the single-valued diabatization, in a given region, is valid as long as $\tau_{12}(q)=n$, where n is an integer—a result known for quite some time.[4–17] As for the three-state diabatization, here we encountered a new condition. We found that a three-state single-valued diabatization, in a given region, is valid if and only if $\omega(q)$, as defined in Eq. (22), is an *integer*.

Before concluding the discussion on these phenomena we would like to briefly relate our work to studies carried out two or three decades earlier on the RT intersections.[4,10,14] Like in our case the main concern in these studies was to use diabatization to eliminate the unpleasant singular NACTs. The function to be used for this purpose has its origin in the electronic eigenfunction $\exp[i\Lambda(\chi-\theta)]$ where χ is an electronic coordinate (with respect to the molecular axis), θ is the corresponding nuclear rotational coordinate, and Λ is an integer.[4,10,14] Following the integration over the electronic coordinates we are left with a NACT of the kind $\exp[-i\Lambda\theta]$ which is reminiscent of the expression we have, i.e., $\exp[i\tau_{12}\theta]$ (in case τ_{12} is a constant). Thus in the two-state case the two approaches are similar as long as the numerical treatment is carried out close enough to the molecular axis. As far as we can tell these earlier studies, when carried out for three states, used different expressions than the ordinary NACTs we apply [see Eq. (20)].

C. The two-shifted-atom configuration

For the two-shifted-atom configuration we distinguish between two situations: (a) the situation where both atoms follow a given contour simultaneously (namely, as a single, rigid body) and (b) the situation where one atom is clamped to its position and the other follows the given contour.

1. The ADT angle and the D matrix for the symmetrical case: Simultaneous (rigid) two-atom rotation

The calculation of the NACTs for a *rigid* rotation of two atoms located at positions $\mathbf{s}_j$; $j=1,2$ is based on the following definition of the derivative for the eigenfunction, $\zeta_k(\mathbf{s}_e|\mathbf{s}_1,\mathbf{s}_2)$ (see also Appendix A):

$$\nabla_{\mathbf{s}}\zeta_k(\mathbf{s}_e|\mathbf{s}_1,\mathbf{s}_2)=\lim_{\Delta\mathbf{s}\to0}\frac{\zeta_k(\mathbf{s}_e|\mathbf{s}_1+\Delta\mathbf{s},\mathbf{s}_2+\Delta\mathbf{s})-\zeta_k(\mathbf{s}_e|\mathbf{s}_1,\mathbf{s}_2)}{\Delta\mathbf{s}}. \tag{24}$$

Consequently the corresponding NACT becomes

$$\tau_{jk}^{(\mathbf{s})}(\mathbf{s}_1,\mathbf{s}_2)=\langle\zeta_j(\mathbf{s}_e|\mathbf{s}_1,\mathbf{s}_2)|\nabla_{\mathbf{s}}\zeta_k(\mathbf{s}_e|\mathbf{s}_1,\mathbf{s}_2)\rangle, \tag{25}$$

where the upper index on the left-hand side indicates that both atoms are shifted simultaneously by an identical differential vectorial amount $\Delta\mathbf{s}$.

Applying these expressions for the case of polar coordinates: (φ_j, q_j); $j=1,2$ we get for the respective angular component the expression

$$\boldsymbol{\tau}_{jk}(\varphi_1,q_1,\varphi_2,q_2) = \left\langle \zeta_j(\mathbf{s}_e|\varphi_1,q_1,\varphi_2,q_2) \left| \frac{\partial}{\partial\varphi}\zeta_k(\mathbf{s}_e|\varphi_1,q_1,\varphi_2,q_2) \right\rangle \right. . \tag{26}$$

Since we treat a rigid rotation of the two atoms, the corresponding NACTs, like in the single atom case, are independent of φ and therefore Eqs. (16)–(23) apply for this case as well.

2. The ADT angle and the topological phase for a single-atom rotation: Theory for the nonsymmetrical case

As is shown in Appendix A the (j,k) NACT in Eq. (25) can be written as a sum of two terms [see Eq. (A7)],

$$\boldsymbol{\tau}_{jk}^{(\mathbf{s})}(\mathbf{s}_1,\mathbf{s}_2) = \boldsymbol{\tau}_{jk}^{(\mathbf{s}_1)}(\mathbf{s}_1,\mathbf{s}_2) + \boldsymbol{\tau}_{jk}^{(\mathbf{s}_2)}(\mathbf{s}_1,\mathbf{s}_2). \tag{27}$$

Equation (27) is, in particular, relevant (but requires additional modifications) for cases where the rotation of the two atoms is not necessarily rigid or when each atom is rotating separately. To continue we write Eq. (27) in terms of cylindrical (polar) coordinates,

$$\boldsymbol{\tau}_{\varphi jk}(q_1,\varphi_1,q_2,\varphi_2) = \boldsymbol{\tau}_{\varphi jk}^{(\varphi_1)}(q_1,\varphi_1,q_2,\varphi_2) + \boldsymbol{\tau}_{\varphi jk}^{(\varphi_2)}(q_1,\varphi_1,q_2,\varphi_2). \tag{28}$$

Equation (28) is used to prove that the ADT angle due to a rigid rotation of two atoms is *approximately* equal to the sum of the two ADT angles, each formed by a separate atom [while following the same (angular) contour, Γ].

To prove this statement we restrict ourselves to the two-state system, return to Appendix A, and consider Eqs. (A8)–(A12), but employ polar coordinates.

The ADT angle γ, due to a rotation of the two rigid atoms along a given contour, Γ, is defined as [see Eq. (A8)]

$$\gamma(\varphi_1,\varphi_2|\varphi_{10},\varphi_{20}|\Gamma) = \int_{(\varphi_{10},\varphi_{20})}^{(\varphi_1,\varphi_2)} \boldsymbol{\tau}_{12}^{(\varphi)}(\varphi_1'\varphi_2'|\Gamma)d\varphi, \tag{29}$$

where φ is not necessarily identical to φ_1' or φ_2' but can be shifted, at most, by a constant [see Eq. (A9)]. From now on q_1 and q_2 are ignored because they are held fixed. The γ angle, due to Eq. (29), can also be written as a sum of two angles [see Eq. (A10)],

$$\gamma(\varphi_1,\varphi_2|\varphi_{10},\varphi_{20}|\Gamma) = \gamma_1(\varphi_1|\varphi_{10},\varphi_{20}|\Gamma) + \gamma_2(\varphi_2|\varphi_{20},\varphi_{10}|\Gamma), \tag{30}$$

where each of the angles is given as a separate line integral [see Eq. (A11)],

$$\gamma_k(\varphi_k|\varphi_{k0},\varphi_{j0}|\Gamma) = \int_{\varphi_{k0}}^{\varphi_k} \boldsymbol{\tau}_{12}^{(\varphi_k)}(\varphi_k',\varphi_j'|\Gamma)d\varphi; \quad j\neq k=1,2. \tag{31}$$

Equation (31) is not yet in the appropriate form so that γ_k can be considered as an ordinary (single atom) ADT angle. In order to achieve that, the second angle in the integrand, i.e., φ_j', has to be replaced by a fixed value, namely, φ_{j0}. Assuming that the two atoms are far apart (in the present study they are ~3.5 Å apart) and that the radii q_1 and q_2 are small enough, we may replace φ_j' by (a fixed) φ_{j0}.

$$\gamma_k(\varphi_k|\varphi_{10},\varphi_{20}|\Gamma) = \int_{\varphi_{k0}}^{\varphi_k} \boldsymbol{\tau}_{12}^{(\varphi_k)}(\varphi,\varphi_{j0}|\Gamma)d\varphi; \quad j\neq k=1,2. \tag{32}$$

Here $\boldsymbol{\tau}_{12}^{(\varphi_k)}(\varphi,\varphi_{j0}|\Gamma)$; $(j,k=1,2$, but $j\neq k)$ is the NACT related to the kth atom while the jth atom is clamped at its position at $\varphi=\varphi_{j0}$.

Following the analysis we performed so far we find that the ADT angle for a rigid rotation of two atoms is approximately given in the form

$$\gamma(\varphi_1,\varphi_2|\varphi_{10},\varphi_{20}|\Gamma) \sim \gamma_1(\varphi_1|\varphi_{10},\varphi_{20}|\Gamma) + \gamma_2(\varphi_2|\varphi_{10},\varphi_{20}|\Gamma), \tag{33}$$

where the ADT angles on the right-hand side of Eq. (33) are given in Eq. (32).

Equations (29)–(33) can also be applied for closed contours so that the following equation is obtained:

$$\alpha(q_1,q_2|\Gamma) \sim \alpha_1(q_1,q_2|\Gamma) + \alpha_2(q_1,q_1|\Gamma), \tag{34}$$

which leads to the following Lemma: *The topological (Berry) phase formed by the rigid motion of two atoms is approximately equal to the sum of the topological phases formed by each atom separately.*

In case the two atoms are identical (and $q_1=q_2=q$) we have $\alpha_1(q)=\alpha_2(q)$ so that

$$\alpha(q) \sim 2\alpha_1(q_1). \tag{35}$$

Equation (35) is of major importance because it leads to the following result:

$$\alpha(q) = 2\pi \Rightarrow \alpha_1(q) = \alpha_2(q) \sim \pi. \tag{36}$$

Equation (36) leads to the following Lemma: *Consider the configuration of two shifted atoms where any rigid rotation around the molecular axis yields the RT topological (Berry) phase i.e., $\alpha=2\pi$. Next let one atom surround this axis while the other atom is clamped. Equation (36) asserts that this rotating atom yields the JT topological (Berry) phase. i.e., $\alpha=\pi$.*

In other words the resulting axis (formed by the two carbons) does not serve as a seam of Renner-Teller degeneracy points as we know them but as a seam for *a kind of* Jahn-Teller degeneracy point. This unexpected (but very reasonable) finding is further discussed following the presentation of numerical results.

III. NUMERICAL RESULTS

In this article is presented a detailed study of the $C_2H_2^+$. Four types of results are discussed: (a) energy curves, (b) nonadiabatic coupling terms, (c) ADT angles and topological phases, and (d) **D**-matrix elements. The calculations are done for three types of configurations as described in Figs. 1(B)–1(D) and as elaborated earlier in the theory chapter, namely, in Secs. II A–II C. Therefore the present chapter is constructed in a similar way. All calculated magnitudes are presented as a function of cylindrical coordinates where the z-coordinates for the four atoms are always *fixed* and therefore are ignored in the discussion.

The calculation of the energy curves and the (angular) NACTs is carried out at the state-average complete active space self-consistent-field (CASSCF) level, employing the following basis functions: For the carbons as well as for the hydrogens we applied s, p, and d functions, all from the aug-cc-pVTZ set. We used the active space, including all nine valence electrons distributed on ten orbitals. Five electronic states, including the three states specifically studied, were computed by the state-average CASSCF level using the 6-311G** basis set with equal weights. In certain cases these calculations were repeated with three/four states to check for convergence. All calculations were done for the following collinear configuration: the C–C distance, $R_{CC}=1.254$ Å and the (two) H–C distances, $R_{HC}=1.080$ Å. The numerical treatment is carried out employing the MOLPRO program.[35]

A. Treatment of the symmetrical case formed by a single shifted hydrogen

A symmetrical case is formed by single shifted hydrogen, which is allowed to rotate along a circle with its center on the triatom axis [see Fig. 1(B)]. In Fig. 2(a) the energy curves are presented as a function of q (the radius of the circle). The two lower curves stand for the two states, $1\,^2A''$ and $1\,^2A'$, that evolve from the collinear $X\,^2\Pi_u$ state, and the third curve is the one that evolves from the collinear $1\,^2\Sigma_g^+$ state and is labeled as $2\,^2A''$.[32(b)] We use this notation to emphasize the fact that A' states interact with A'' states and therefore $1\,^2A'$ is expected to interact with both $1\,^2A''$ and $2\,^2A''$. This of course does not apply to the $1\,^2A''$ state which interacts only with the $1\,^2A'$ state but not with the $2\,^2A''$ state (thus the NACT term between these two states is identically zero).

Since the $1\,^2A'$ and $1\,^2A''$ curves in Fig. 2 are hardly distinguishable they are presented again in Fig. 2(b) where the energy scale is decreased so that the two curves are more distinguishable. The energy difference between the two energy curves is presented in the insert, to provide a better view of how these two curves evolve as q increases. It can be seen that the $1\,^2A'$ curve is above the $1\,^2A''$ curve along the interval $q\sim\{0.0-0.905\}$ Å but then the two intersect (at the point $\oplus$) and the order of the two curves is reversed. This intersection takes place without the formation of topological effects or any other types of potential coupling. In other words it is immaterial what happens these two curves continue to be transparent to each other. In Appendix B this situation is analyzed mathematically and the consequences of such an intersection are summarized.

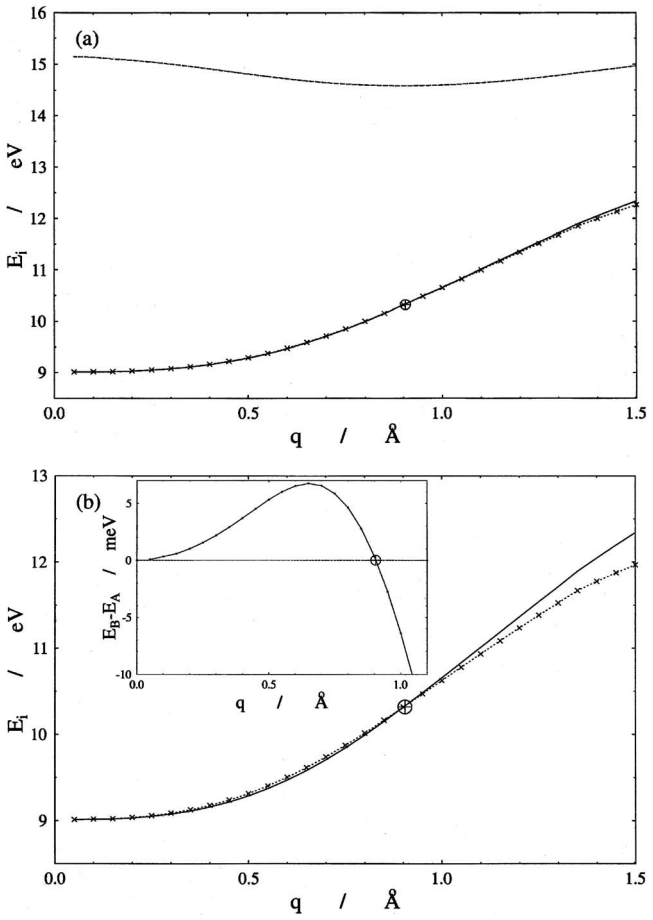

FIG. 2. Energy curves as a function of q (for the single-atom symmetric case) related to three electronic states: the $1\,^2A'$ state, the $1\,^2A''$ state (both evolving from the two degenerate $X\,^2\Pi_u$ state), and the state which evolves from the (collinear) Σ state to become the $2\,^2A''$ state. These three states are the lower ones for the collinear arrangement and at regions close to it. (a) The three energy curves: (···+···+···+··) $E_{1A'}(q)$; (———) $E_{1A''}(q)$; (-----) $E_{2A''}(q)$. The symbol $\oplus$ indicates the position of the intersection point between the two curves. (b) The two lower curves $E_{1A'}(q)$ and $E_{1A''}(q)$; for a reduced scale. In the insert is given the energy difference $=[E_{1A'}(q)-E_{1A''}(q)]$. It is noticed that at the point $\oplus$ this difference flips its sign.

Figure 3(a) presents the three NACTs: $\tau_{12}(q)$, $\tau_{13}(q)$, and $\tau_{23}(q)$. It can be clearly seen that $\tau_{12}(q)$ differs from zero along the whole studied interval. The only unusual behavior to be seen is the sudden sign flip at $q\sim0.905$ Å which is caused by the change of the order of the curves at the intersection point (as explained above).

Another phenomenon that takes place at the intersection point is the switch of roles between $\tau_{23}(q)$ with $\tau_{13}(q)$. Along the interval $\{0.0-0.905\}$ Å the two states $1\,^2A'$ and $2\,^2A''$ are coupled by $\tau_{23}(q)$ but along the interval $q>0.905$ Å, due to the switch of the two states $1\,^2A'$ and $1\,^2A''$, the same two states are coupled by $\tau_{13}(q)$. In Fig. 3(b) are presented the two coupling terms: the upper curve stands for $\tau_{12}(q)$, which couples $1\,^2A'$ and $1\,^2A''$ (and ignores the sign flip), and the lower curve, which is due to the two terms $\tau_{23}(q)$ and $\tau_{13}(q)$ that couple $1\,^2A'$ and $2\,^2A''$ (as explained).

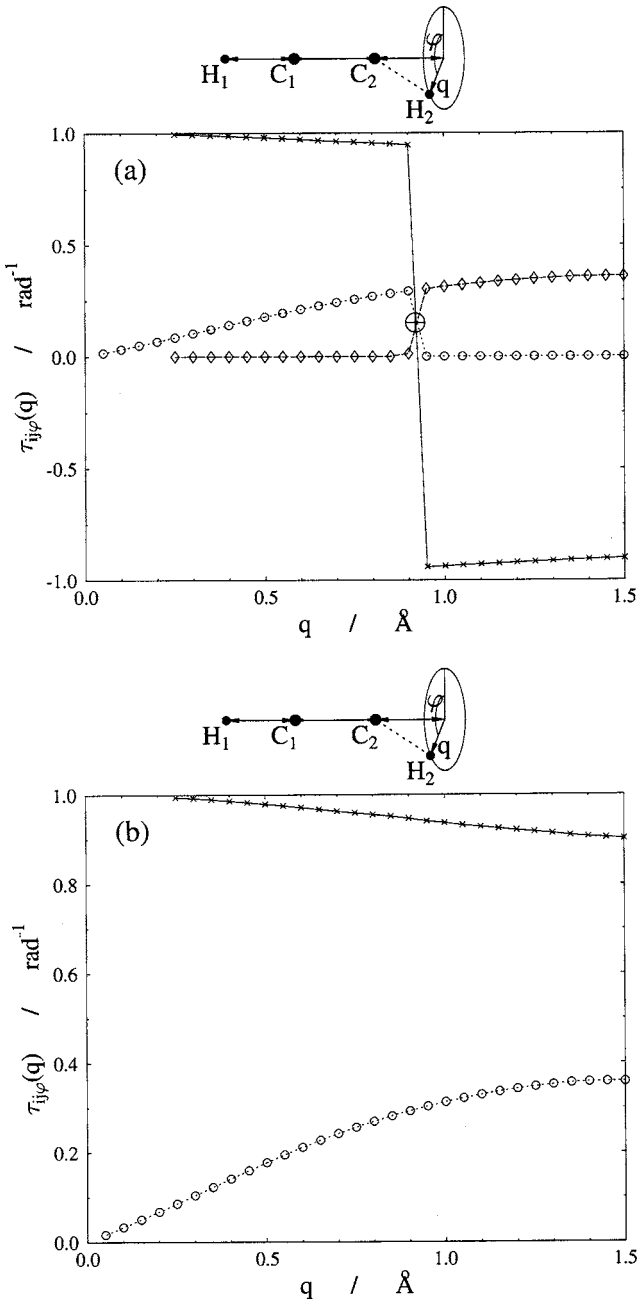

FIG. 3. *Ab initio* q-dependent RT nonadiabatic coupling terms (for the single-atom symmetric case): (a) (××××) $\boldsymbol{\tau}_{\varphi 12}(q)$; (○○○○) $\boldsymbol{\tau}_{\varphi 23}(q)$; (◇◇◇◇) $\boldsymbol{\tau}_{\varphi 13}(q)$. The symbol ⊕ indicates the position of the intersection point between $E_{A'}(q)$ and $E_{A''}(q)'$ (see Fig. 2). (b) (××××) $\boldsymbol{\tau}_{12}(q)$ (after removing the sign flip); (○○○○) $\boldsymbol{\tau}_{23}(q)$ (the physical NACT that couples $1\,^2A'$ and $2\,^2A''$ along the whole considered interval). These two NACTs are used for the calculations of the **D**-matrix elements (presented in Fig. 4).

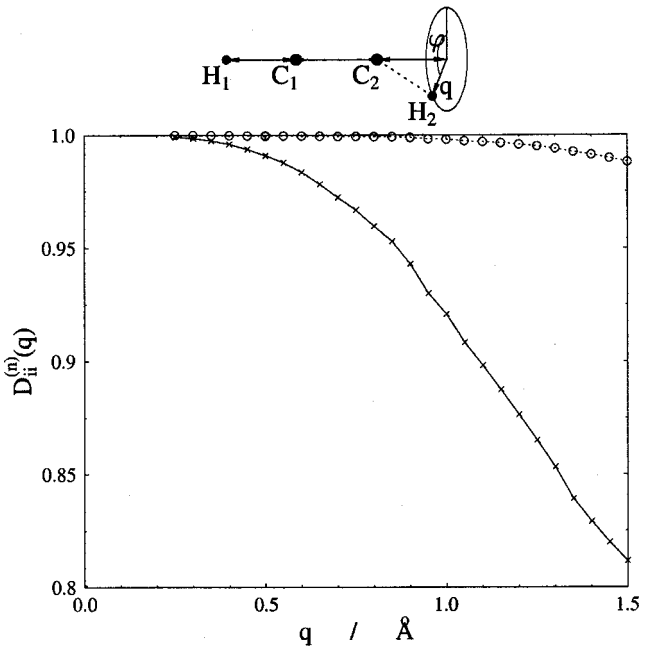

FIG. 4. The two-state and the three-state **D**-matrix elements: Two curves are shown, one represents the (1,1) elements of $\mathbf{D}^{(2)}$ and one represents the (1,1) elements of $\mathbf{D}^{(3)}$: (××××) $\mathbf{D}^{(2)}_{11}(q)$; (○○○○) $\mathbf{D}^{(3)}_{11}(q)$.

In Fig. 4 are presented the diagonal **D**-matrix elements. One curve presents these elements for the two-state case and the other for the three-state case. We remind the reader that in order to have a *single-valued* diabatization the **D** matrix has to be diagonal and its elements have to be equal to 1. In other words the **D** matrix has to be the unit matrix.

We start the analysis for the two-state case. Following Eq. (17) we note that, always, $D_{11}(q)=D_{22}(q)$ (and therefore only one curve is presented). It is clearly seen that the values of $D_{11}(q)$ are equal to 1 only along a short q range ($q \leqslant 0.3$ Å) and from there on the deviations increase significantly as q gets larger. Thus at $q \sim 1.5$ Å the value of $D_{11}(q)$ is ~0.80. The reason is the deterioration of $\boldsymbol{\tau}_{12}(q)$ which is expected to be 1 but, in fact, is ~0.9 [see Fig. 3(b)].

A more encouraging situation follows when we consider three states. Again only one curve is presented because all three curves related to $D_{jj}(q) \sim 1$; $j=1,2,3$ almost coalesce along most of the studied interval and are ~1. In other words the three-state **D** matrix is very close to being a *unit* matrix. From Eq. (23) it can be seen that in order for that to happen the value of ω defined as

$$\omega = \sqrt{\boldsymbol{\tau}_{12}^2 + \boldsymbol{\tau}_{23}^2} \tag{37}$$

has to be an ~ integer, i.e., $\omega \sim n$.

Summary. In this study we showed that in order to carry out dynamical calculations for a case of a shifted hydrogen we have to consider at least three states in order to guarantee *single-valued* diabatic potential energy surfaces along the whole mentioned interval (~1.5 Å). A two-state diabatization is valid for only a short interval (<0.3 Å).

B. Treatment of symmetrical case formed by a pair of (rigid) atoms

As already mentioned earlier this symmetrical case (namely, the case where both the potential energy surfaces and the NACTs are independent of the angle φ) is formed by rotating the two hydrogens as a single rigid body [see Fig. 1(C)]. Consequently the only independent variables are q_1 and q_2. In the present article we refer to the case that $q_1 = q_2 (= q)$.

In Fig. 5(a) are presented five potential energy curves as a function of q: The two lower curves, i.e., $E_{A1}(q)$ and $E_{B1}(q)$, stand for the states $1\,^2A_1$ and $1\,^2B_1$, respectively, that evolve from the collinear $X\,^2\Pi_u$ state. The three additional curves E_{A2}, $E_{B2}(q)$, and $E_{A3}(q)$ stand for the $1\,^2A_2$ state

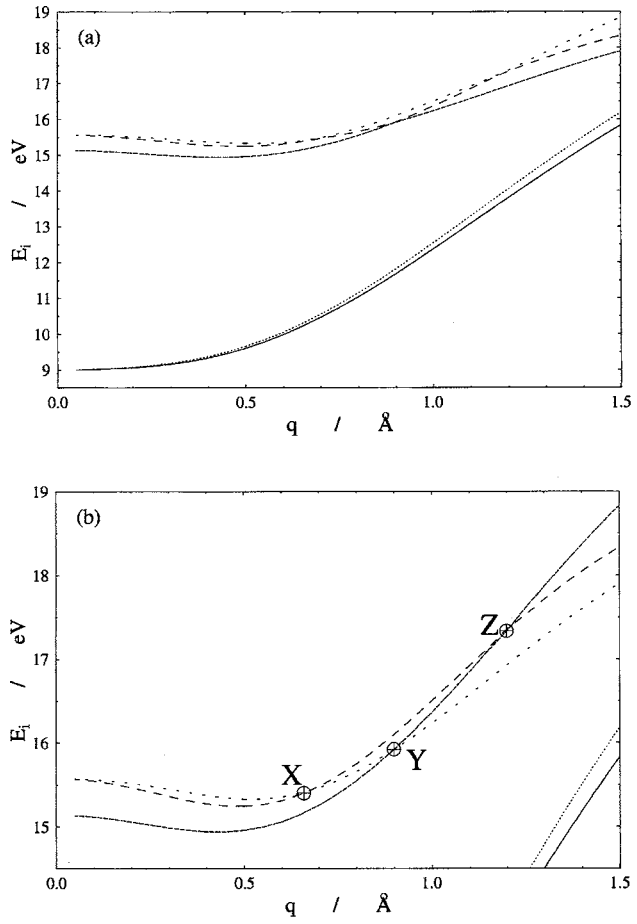

FIG. 5. Energy curves as a function of q [for the (rigid) two-atom symmetric case] related to five electronic states, namely, $1\,^2B_1$ and $1\,^2A_1$ (evolving from the $X\,^2\Pi_u$ state) the $1\,^2A_2$ state evolving from the collinear Σ state and the $1\,^2B_2$ and the $2\,^2A_1$ state (evolving the $1\,^2\Pi_g$ state). These five states are the lower ones for the collinear arrangement and at regions close to it. (a) The five *adiabatic* energy curves; (b) the three upper (physical) RT energy curves (----------) $E_{A2}(q)$, (----) $E_{B2}(q)$;(· · · · · · · · ·) $E_{A3}(q)$; the letters X, Y, and Z indicate the intersection points between $E_{B2}(q)$ and $E_{A3}(q)$ between $E_{A3}(q)$ and $E_{A2}(q)$ and between $E_{B2}(q)$ and $E_{A2}(q)$, respectively. On the right lower corner are seen segments of the two lower RT energy curves: (· · · · · · · · ·) $E_{B1}(q)$; (—) $E_{A1}(q)$.

(which evolves from the collinear Σ state) and the $1\,^2B_2$ and $2\,^2A_1$ states that evolve from the $1\,^2\Pi_g$ state. Whereas the two lower curves run parallel to each other and do not intersect [$E_{B1}(q)$ is always the upper curve], the next three curves intersect each other several times and cause difficulties in identifying the various states (we remind the reader that these intersections are not accompanied by topological phenomena or other types of coupling—see analysis in Appendix B).

In Fig. 5(b) we concentrate on the three upper curves in order to identify them (using the corresponding NACTs as is explained next). It is now noticed that $E_{A2}(q)$ is the lowest curve along the interval {0.0–0.905} Å but it then intersects the $E_{A3}(q)$ curve at point Y and later the $E_{B2}(q)$ curve at point Z. We also notice that along the interval {0.0–0.6} Å the curve $E_{A3}(q)$ is above $E_{B2}(q)$ but they switch positions after the intersection at point X.

In Fig. 6(a) are presented the corresponding NACTs $\tau_{12}(q)$, $\tau_{23}(q)$, $\tau_{24}(q)$, and $\tau_{25}(q)$. Whereas the situation with

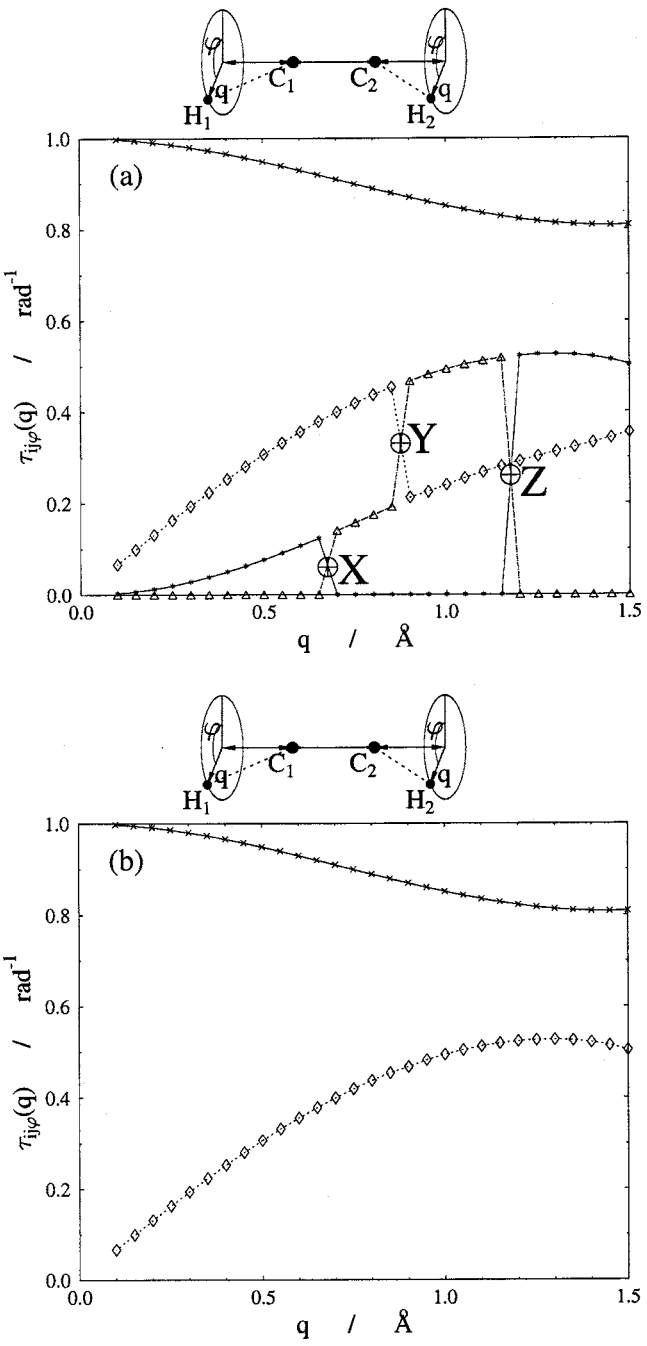

FIG. 6. *Ab initio* q-dependent RT nonadiabatic coupling terms [for the (rigid) two-atom symmetric case]: (a) (××××) $\tau_{\varphi 12}(q)$; (◇◇◇◇) $\tau_{\varphi 23}(q)$; (△△△△) $\tau_{\varphi 24}(q)$; (· · ·); for the meaning of X, Y, and Z see Fig. 5(b). (b) (××××) $\tau_{12}(q)$; (○○○○) $\tau_{23}(q)$ (the physical NACT that couples $1\,^2B_1$ and $1\,^2A_2$ along the whole considered interval). These two NACTs are used for the calculations of the **D**-matrix elements (presented in Fig. 7).

regard to $\tau_{12}(q)$ is clear and does not require any additional explanation, the situation with regard to the other three NACTs is somewhat confusing. If we ignore what happens at the intersection points X, Y, and Z it is seen that the three NACTs $\tau_{23}(q)$, $\tau_{24}(q)$, and $\tau_{25}(q)$ form a kind of two continuous curves. The upper curve is formed, along the interval q={0.0–0.905} Å by $\tau_{23}(q)$, along the interval q ={0.905–1.15} Å by $\tau_{24}(q)$, and along the interval q ={1.15–1.5} Å by $\tau_{25}(q)$. In the same way the lower curve is

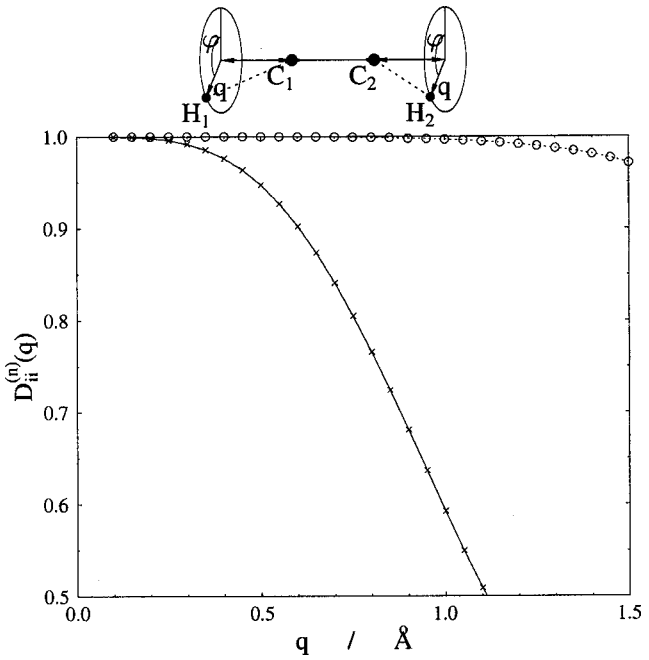

FIG. 7. The two-state and the three-state **D**-matrix elements for the (rigid) two-atom symmetrical case: (××××) $\mathbf{D}_{11}^{(2)}(q)$ [represents the (1,1) elements of the $\mathbf{D}^{(2)}$ matrix]; (○○○○) $\mathbf{D}_{11}^{(3)}(q)$ [represents the (1,1) elements of the $\mathbf{D}^{(3)}$ matrix].

formed along the interval $q=\{0.0-0.65\}$ Å by $\tau_{25}(q)$, along the interval $q=\{0.65-0.905\}$ Å by $\tau_{24}(q)$, and along the interval $q=\{0.905-1.5\}$ Å by $\tau_{23}(q)$. It is quite clear that the above switches are caused by the intersections of the three energy curves and therefore the two resulting NACT curves are in fact, the NACT between $1\,^2B_1$ and $1\,^2A_2$ (upper curve) and between $1\,^2B_1$ and $2\,^2A_1$ (lower curve).

In Fig. 6(b) are presented the two NACTs that are relevant for the present study. As previously mentioned the upper curve presents $\tau_{12}(q)$, and the lower curve presents the coupling term between states $1\,^2B_1$ and $1\,^2A_2$ which, for the forthcoming applications, is (redefined and) designated as $\tau_{23}(q)$.

Next we briefly refer to the two-state and three-state **D**-matrix elements. These elements are presented in Fig. 7 and we encounter a similar situation as in the single rotating atom case (see Fig. 4) with one exception. On the one hand the deterioration of the *two-state* (diagonal) **D**-matrix element is much faster in the present case, and therefore it reaches smaller values (0.5 as compared to 0.8 in the single-atom case). On the other hand the three-state (diagonal) **D**-matrix element is as stable as in the single atom case and is ~1 along the whole interval.

Short summary. In this study we showed that in order to form a single-valued diabatic potential matrix for a case where *two* rigid hydrogens are shifted from the collinear axis in most cases we have to consider at least three states.

C. Treatment of the nonsymmetrical case

The nonsymmetrical case is described in Fig. 1(D) and results are presented in Figs. 8 and 9. Here we treat a situation where the two carbons (as before) form the axis, one off-axis hydrogen is clamped at a distance q_1 from this axis

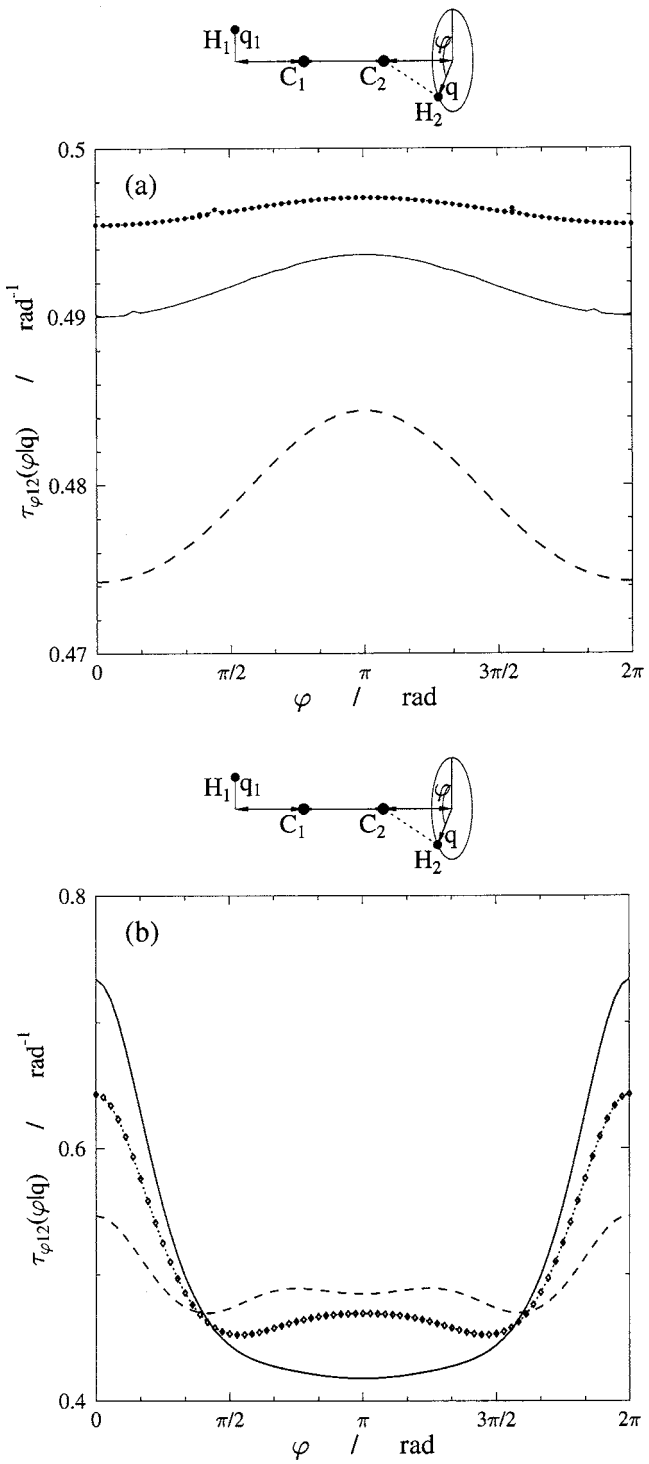

FIG. 8. *Ab initio* φ-dependent RT nonadiabatic coupling term, $\tau_{12}(\varphi|q_1,q_2)$, for the single-atom, nonsymmetric case [see case (D) in Fig. 1]: (a) Results for the case $q_1=q_2(=q)$; (•••••) $q=0.2$ Å; (—) $q=0.3$ Å; (---) $q=0.5$ Å. (b) Results for $q_1\neq q_2(=q)$: (---) ($q_1=0.3$, $q=0.5$ Å); (—) ($q_1=0.1$, $q_2=0.5$ Å); (◇◇◇◇) ($q_1=0.1$, $q_2=0.8$ Å).

while the other off-axis hydrogen, at a distance q, is allowed to surround the axis. In this way we create a situation where the NACTs, due to the (single) surrounding atom, depend not only on (q_1,q_2) but also on the angle φ, which is the angle between two planes, CCH1 and CCH2. However, it is also expected that the larger the distance between these two hydrogens the weaker is this dependence.

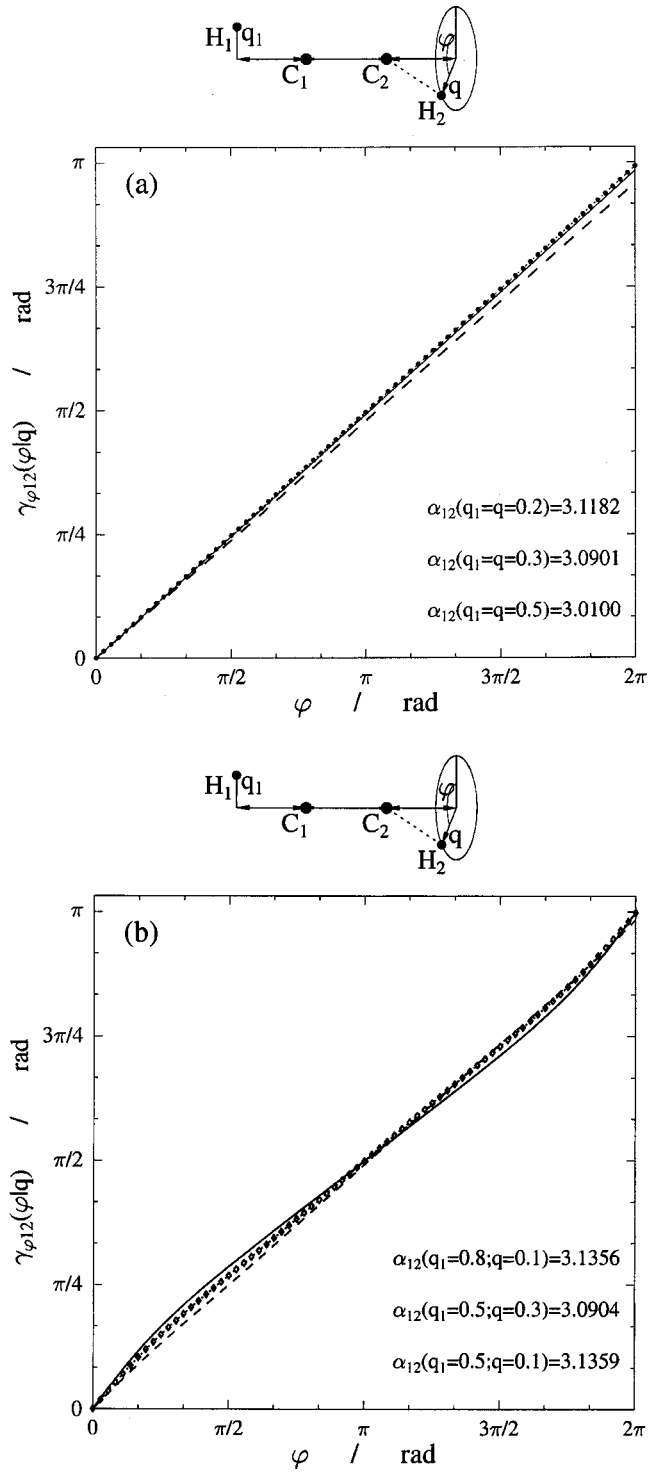

FIG. 9. φ-dependent RT ADT angle, $\gamma(\varphi|q_1,q_2)$ as calculated for the single-atom, nonsymmetric case [see case (D) in Fig. 1]: (a) Results for the case $q_1=q_2(=q)$; (•••••) $q=0.2$ Å; (—) $q=0.3$ Å; (---) $q=0.5$ Å. (b) Results for $q_1\neq q(=q_2)$: (---) $q=0.3$, $q_1=0.5$ Å; (——) $q=0.1$, $q_1=0.5$ Å; ($\diamond\ \diamond\ \diamond\ \diamond$) $q=0.1$, $q_1=0.8$ Å. At the bottom of each subfigure are listed values of the corresponding topological (JT) phases $\alpha(q)$ and $\alpha(q_1,q)$, respectively.

In this section we concentrate on energy curves, NACTs and ADT angles, related to the two lower states, $1\,^2A''$ and the $1\,^2A'$, calculated only as a function of φ for several combinations of (q_1,q_2). On this occasion we remind the reader that along the collinear configuration the following distances were assumed: $R_{CC}=1.254$ Å and $R_{HC}=1.080$ Å.

We start the analysis with the energy curves. In fact, we do not show any results because we find, somewhat to our surprise, that all the energy curves are *independent* of φ (or at most slightly dependent on φ). In other words they are symmetric with regard to the C–C axis although the shifted clamped atom H1 is expected to yield nonsymmetrical energy curves. The only explanation for this finding is that as far as the energy curves are concerned H1 is too far from H2 $(=(R_{CC}+2R_{HC})\geqslant 3.41$ Å) and therefore the nonsymmetric structure essentially disappears. This result is also supported by other studies.[17]

In Fig. 8 are presented NACTs and they show some dependence on φ. In Fig. 8(a) are presented NACTS for which $q_1=q_2(=q)$ and in Fig. 8(b) are presented NACTs for which $q_1\neq q$ $(=q_2)$. In Fig. 8(a) are shown three curves as calculated for $q=0.2$, 0.3, 0.5 Å. It is noticed that the curves oscillate to some extent in the vicinity of the value $\tau_{12}(q)\sim 0.5$ rad^{-1}. As q decreases the curves become less oscillatory and tend to approach the value $\tau_{12}(q)=0.5$ rad^{-1}. In Fig. 8(b) are shown three curves as calculated for $(q_1,q)\equiv(0.5,0.3);(0.5,0.1);(0.8,0.1)$ Å. It is noticed that in general the curves keep their values close to $\tau_{12}(q)\sim 0.5$ rad^{-1} and are weakly dependent on φ. It turns out that more can be said about these NACTs but this will be done in a subsequent publication.

Next we refer to the ADT angles $\gamma(\varphi|q_1,q_2)$ as calculated employing Eq. (12) [see also Eq. (32)]. These are presented in Fig. 9 for the case that $\varphi_{10}=\varphi_{20}=0$. In Fig. 9(a) are presented the $\gamma(\varphi|q)$ angles for the cases that $(q_1=q_2=)$ $q=0.2,0.3,0.5$ Å and in Fig. 9(b) are presented the angles $\gamma(\varphi|q_1,q_2)$ for the above-mentioned three cases for which $q_1\neq q_2$ $(=q)$. It is noticed that all the curves are monotonic increasing functions of φ that start at $\gamma=0$ and become $\gamma\sim\pi$ once $\varphi=2\pi$, irrespective of the values of q_1 and q. This result implies that the topological phase, $\alpha(q_1,q_2)$, in all studied cases is $\sim\pi$, as expected for Jahn-Teller intersections

The actual values of $\alpha(q_1,q_2)$ are listed in Figs. 9(a) and 9(b) and it can be seen that all of them are, indeed, close to π. In addition we notice that the smaller the value of q $(=q_2)$, the closer is the value of $\alpha(q_1,q_2)$ to π. Thus, whereas for $q=0.5$ Å we have the lowest value for α, i.e., $\alpha=3.01$ we get for $q=0.1$ Å the value $\alpha=3.12$ which is much closer to π $(=3.14)$. At the same time one notices that the dependence on q_1 [as opposed to q_2 $(=q)$] is relatively weak.

In Sec. II C 2 we studied, theoretically, the nonsymmetrical case and we were able to show that for the case $q_1=q$ the corresponding topological phase is $\alpha(q)\sim\pi$ [see Eq. (36)]. The numerical treatment indicates a more general result, namely, that as long as both q_1 and q_2 differ from zero the topological phase is $\sim\pi$. However, if either q_1 or q_2 becomes zero the corresponding topological phase changes *abruptly* and becomes 2π.

IV. CONCLUSIONS

The study presented in this article can be considered as a continuation of a previous study carried out for the triatom HNH molecule.[2] Although it is a tetra-atomic system, still most of the findings that were revealed for the triatom sys-

tem apply here as well. In particular, the present study strengthened the importance of the **D** matrix for the study of the diabatization process.

The fact that a tetra-atomic system provides additional possibilities makes the study of such a molecule more interesting. In the case of a triatomic system, topological effects are revealed when one atom surrounds the axis formed by the two other atoms.[2] In the case of tetra-atomic systems, topological effects are revealed when one atom surrounds the triatom axis or when two atoms surround (at a time) the *two-atom axis*. In other words it is shown that for a tetra-atomic system not only a triatom axis but even a two-atom axis forms a *seam* that contains degeneracy points. This finding can be expressed also in a third way, namely, shifting away two atoms from the collinear axis is not enough to *abolish* the topological effects produced by the original triatom axis. This feature probably can be found in larger collinear molecules where a group of n atoms ($n>2$) are allowed to surround an axis formed by the remaining atoms.

We already know that along the collinear axis of the tetra-atomic molecule are distributed poles (or degeneracy points) responsible for the RT effect. However, in the present study we revealed an additional phenomenon, namely, that the same axis (or nearby lines that run parallel to it) serves also as a source for poles that produce JT effects. These are formed when two atoms are shifted away from the collinear axis but only one atom is allowed to surround this axis, whereas the other is clamped to its position [see Fig. 1(D)]. These are *pseudo* JT effects because the intersections that lead to these effects are between A' and A'' states and not like in the case of the ordinary JT effect which is produced by two states with the same symmetry. Still the topological (Berry) phase is π and not 2π. This rather surprising finding requires more study that will be reported in one of our forthcoming articles.

In conclusion, in this study we exposed one of the more dramatic features in quantum chemistry, namely, the abrupt transition from a Jahn-Teller intersection to a Renner-Teller intersection (or vice versa), both formed *along* the same *seam*.

ACKNOWLEDGMENTS

The authors acknowledge the US-Israel Bi-national Science Foundation for partly supporting this study. One of the authors (A.V.) acknowledges OTKA Grant Nos. T037994 and M041537, and the computational resources provided by the John-von-Neumann Institute, Research Centre Juelich. One of the authors (D.J.K.) acknowledges the R. A. Welch Foundation, Grant No. E-0608.

APPENDIX A: DERIVATION OF THE NACTs AND THE ADT ANGLE FOR TWO SHIFTED RIGID AND NONRIGID ATOMS

Assume two atoms P1 and P2 connected rigidly to each other, located at points $\mathbf{s}_1$ and $\mathbf{s}_2$. We start with the general definition of the (j,k) NACT, $\boldsymbol{\tau}_{jk}^{(s)}(\mathbf{s})$

$$\boldsymbol{\tau}_{jk}^{(s)}(\mathbf{s}) = \langle \zeta_j(\mathbf{s}_e|\mathbf{s}) | \nabla_{\mathbf{s}} \zeta_k(\mathbf{s}_e|\mathbf{s}) \rangle, \tag{A1}$$

where the grad operator stands for a vectorial differentiation with respect to the nuclear coordinates $\mathbf{s}$ ($\mathbf{s}_e$ is the electronic coordinate). In the case of two rigid atoms located at $\mathbf{s}_1$ and $\mathbf{s}_2$ this differentiation takes the form

$$\nabla_{\mathbf{s}} \zeta_k(\mathbf{s}_e|\mathbf{s}_1,\mathbf{s}_2) + \lim_{\Delta s \to 0} \frac{\zeta_k(\mathbf{s}_e|\mathbf{s}_1+\Delta\mathbf{s},\mathbf{s}_2+\Delta\mathbf{s}) - \zeta_k(\mathbf{s}_e|\mathbf{s}_1,\mathbf{s}_2)}{\Delta\mathbf{s}}, \tag{A2}$$

so that the corresponding NACT becomes

$$\boldsymbol{\tau}_{jk}^{(s)}(\mathbf{s}_1,\mathbf{s}_2) = \langle \zeta_j(\mathbf{s}_e|\mathbf{s}_1,\mathbf{s}_2) | \nabla_{\mathbf{s}} \zeta_k(\mathbf{s}_e|\mathbf{s}_1,\mathbf{s}_2) \rangle. \tag{A3}$$

Next it is shown that this NACT can be presented as the sum of two NACTs where each NACT is related to one of the atoms. For this purpose we add to the denominator in Eq. (A2) two identical terms with opposite signs,

$$\therefore \lim_{\Delta\mathbf{s}\to 0} \left\{ \frac{\zeta_k(\mathbf{s}_e|\mathbf{s}_1+\Delta\mathbf{s},\mathbf{s}_2+\Delta\mathbf{s}) - \zeta_k(\mathbf{s}_e|\mathbf{s}_1,\mathbf{s}_2+\Delta\mathbf{s})}{\Delta\mathbf{s}} + \frac{\zeta_k(\mathbf{s}_e|\mathbf{s}_1,\mathbf{s}_2+\Delta\mathbf{s}) - \zeta_k(\mathbf{s}_e|\mathbf{s}_1,\mathbf{s}_2)}{\Delta\mathbf{s}} \right\}. \tag{A4}$$

Without losing the generality, Eq. (A4) can be written also as

$$\therefore \lim_{\substack{\Delta\mathbf{s}_1\to 0 \\ \Delta\mathbf{s}_2\to 0}} \left\{ \frac{\zeta_k(\mathbf{s}_e|\mathbf{s}_1+\Delta\mathbf{s}_1,\mathbf{s}_2+\Delta\mathbf{s}_2) - \zeta_k(\mathbf{s}_e|\mathbf{s}_1,\mathbf{s}_2+\Delta\mathbf{s}_2)}{\Delta\mathbf{s}_1} + \frac{\zeta_k(\mathbf{s}_e|\mathbf{s}_1,\mathbf{s}_2+\Delta\mathbf{s}_2) - \zeta_k(\mathbf{s}_e|\mathbf{s}_1,\mathbf{s}_2)}{\Delta\mathbf{s}_2} \right\}. \tag{A5}$$

Activating the limit process on the first term with respect to $\Delta\mathbf{s}_2$ and on the second term with respect to $\Delta\mathbf{s}_1$, Eq. (A5) simplifies as follows:

$$\therefore \lim_{\Delta\mathbf{s}_1\to 0} \frac{\zeta_k(\mathbf{s}_e|\mathbf{s}_1+\Delta\mathbf{s}_1,\mathbf{s}_2) - \zeta_k(\mathbf{s}_e|\mathbf{s}_1,\mathbf{s}_2)}{\Delta\mathbf{s}_1} + \lim_{\Delta\mathbf{s}_2\to 0} \frac{\zeta_k(\mathbf{s}_e|\mathbf{s}_1,\mathbf{s}_2+\Delta\mathbf{s}_2) - \zeta_k(\mathbf{s}_e|\mathbf{s}_1,\mathbf{s}_2)}{\Delta\mathbf{s}_2}, \tag{A6}$$

so that we finally get

$$\boldsymbol{\tau}_{jk}^{(s)}(\mathbf{s}_1,\mathbf{s}_2) = \boldsymbol{\tau}_{jk}^{(s_1)}(\mathbf{s}_1,\mathbf{s}_2) + \boldsymbol{\tau}_{jk}^{(s_2)}(\mathbf{s}_1,\mathbf{s}_2). \tag{A7}$$

In what follows we show that the ADT angle γ due to a motion of the two rigid atoms along a given contour is equal to the sum $\gamma_1+\gamma_2$ where γ_1 and γ_2 are calculated, independently.

The ADT angle γ, due to a motion of the two rigid atoms along a given contour, is defined as

$$\gamma(\mathbf{s}_1,\mathbf{s}_2|\mathbf{s}_{10},\mathbf{s}_{20}|\Gamma) = \int_{(\mathbf{s}_{10},\mathbf{s}_{20})}^{(\mathbf{s}_1,\mathbf{s}_2)} \boldsymbol{\tau}_{12}^{(s)}(\mathbf{s}_1',\mathbf{s}_2')\mathbf{ds}, \tag{A8}$$

where in general $\mathbf{s}_k'=\mathbf{s}_k'(\mathbf{s})$, but in our particular case

$$\mathbf{s}_k' = \mathbf{s} + \mathbf{s}_{k0}; \quad k=1,2. \tag{A9}$$

Equation (A8) can also be written as [see Eq. (A7)]

$$\gamma(\mathbf{s}_1,\mathbf{s}_2|\mathbf{s}_{10},\mathbf{s}_{20}|\Gamma) = \int_{\mathbf{s}_{10}}^{\mathbf{s}_1} \boldsymbol{\tau}_{12}^{(\mathbf{s}_1)}(\mathbf{s}_1',\mathbf{s}_2') \cdot \mathbf{ds} + \int_{\mathbf{s}_{20}}^{\mathbf{s}_2} \boldsymbol{\tau}_{12}^{(\mathbf{s}_2)}(\mathbf{s}_2',\mathbf{s}_1') \cdot \mathbf{ds}. \tag{A10}$$

Writing the angle γ as a sum of two angles

$$\gamma(\mathbf{s}_1,\mathbf{s}_2|\mathbf{s}_{10},\mathbf{s}_{20}|\Gamma) = \gamma_1(\mathbf{s}_1|\mathbf{s}_{10},\mathbf{s}_{20}|\Gamma) + \gamma_2(\mathbf{s}_2|\mathbf{s}_{20},\mathbf{s}_{10}|\Gamma), \tag{A11}$$

it is straightforward to notice [recalling Eq. (A10)] that γ_1 and γ_2 are given as follows:

$$\gamma_k(\mathbf{s}_k|\mathbf{s}_{k0},\mathbf{s}_{j0}|\Gamma) = \int_{\mathbf{s}_{k0}}^{\mathbf{s}_k} \boldsymbol{\tau}_{12}^{(\mathbf{s}_k)}(\mathbf{s}_k',\mathbf{s}_j') \cdot \mathbf{ds}; \quad j \neq k = 1,2. \tag{A12}$$

Here $\boldsymbol{\tau}_{12}^{(\mathbf{s}_k)}(\mathbf{s}_k,\mathbf{s}_j)$; $(j,k=1,2$ but $j \neq k)$ is the NACT related to the kth atom while the j atom is at $\mathbf{s}_j$.

APPENDIX B: ON THE NONTOPOLOGICAL DEGENERACY

The connection between the NACTs and typical molecular magnitudes is given in the form[36]

$$\boldsymbol{\tau}_{jk} = \frac{\langle \zeta_j | \nabla \mathbf{H}_e | \zeta_k \rangle}{u_k - u_j}. \tag{B1}$$

In what follows we briefly elaborate on the meaning of Eq. (B1) particularly in the vicinity of a degeneracy point. In order to do that in a simple way, we consider a molecular system characterized by a line of degeneracy points. Next we define a plane which does not contain the line and consider a contour in this plane that surrounds the line. Assuming Ω, as the intersection point of the line with the plane, this contour also surrounds Ω. To continue we define on this plane a system of coordinates—with its origin at Ω—so that any point, P, on this plane is defined in terms of two polar coordinates (q,φ), where q measures the distance between P and Ω. In what follows we concentrate on the angular component of Eq. (B1). Since the angular component of $\boldsymbol{\tau}$ is $\boldsymbol{\tau}_\varphi/q$ and the angular component of the grad operator is $(1/q)(\partial/\partial\varphi)$, the angular component can be written in the form

$$\frac{1}{q}\boldsymbol{\tau}_{\varphi jk} = \frac{1}{q}\frac{\langle \zeta_j | \partial/\partial\varphi \mathbf{H}_e | \zeta_k \rangle}{u_k - u_j}. \tag{B2}$$

Next we assume that $u_k(q,\varphi)$ and $u_j(q,\varphi)$ behave at the vicinity of $q \sim 0$, in the following way:

$$\lim_{q\to 0} u_i \sim u_0(\varphi) + \lambda_i(\varphi)q^m + O(q^{m+1}); \quad i = j,k, \tag{B3}$$

where m is an integer and $u_0(\varphi)$ and $\lambda_i(\varphi)$; $i=j,k$ are analytic functions. In the same way we assume that

$$\lim_{q\to 0} \left\langle \zeta_j \left| \frac{\partial}{\partial\varphi} \mathbf{H}_e \right| \zeta_k \right\rangle \sim \eta_{jk}(\varphi)q^n + O(q^{n+1}), \tag{B4}$$

where $\eta_{jk}(\varphi)$ is an analytic function of φ. In order for the expression in Eq. (B2) to be a pole we have to have $m=n$ and indeed in cases where a Jahn-Teller or a Renner-Teller intersection is encountered we expect this equality to be fulfilled. However, if $n>m$ no pole is encountered at Ω which implies that $\boldsymbol{\tau}_\varphi \equiv 0$.

At this stage we make two comments: (1) At the above defined point Ω we may encounter a JT or a RT degeneracy. The JT effect is formed by a *seam* not located in the plane of the molecule and therefore the contour chosen to surround this seam can be assumed to be in the plane. In the same way the RT effect is usually formed by a *seam* located in the plane of the molecule (e.g., the axis of the molecule) and therefore the contour chosen to surround this seam has to be outside of the plane. (2) Therefore at the point Ω the relation $n=m$ can be satisfied for the JT intersection (and then we have a JT topological effect) but not necessarily for the RT intersection, which means that the intersection does not yield a RT topological effect.

[1] G. J. Halász, Á. Vibók, R. Baer, and M. Baer, J. Chem. Phys. **124**, 081106 (2006).
[2] G. J. Halász, Á. Vibók, R. Baer, and M. Baer, J. Chem. Phys. **125**, 094102 (2006).
[3] M. Baer, *Beyond Born Oppenheimer; Electronic Non-Adiabatic Coupling Terms and Conical Intersections* (Wiley, Hoboken, NJ, 2006), Chaps. 4 and 5.
[4] M. Peric and S. Peyerimhoff, Adv. Chem. Phys. **124**, 583 (2002).
[5] E. Renner, Z. Phys. **92**, 172 (1934).
[6] G. Herzberg, *Molecular Spectra and Molecular Structure Vol. III* (Krieger, Malabar, 1991).
[7] H. C. Longuet-Higgins, Adv. Spectrosc. (N.Y.) **2**, 429 (1961).
[8] K. Dressler and D. A. Ramsay, J. Chem. Phys. **27**, 971 (1957); Philos. Trans. R. Soc. London, Ser. A **251**, 553 (1958).
[9] J. A. Pople and H. C. Longuet-Higgins, Mol. Phys. **1**, 372 (1958).
[10] Ch. Jungen and A. J. Merer, Mol. Phys. **40**, 1 (1980); **40**, 95 (1980); Ch. Jungen and A. J. Merer, in *Molecular Spectroscopy, Modern Research*, edited by K. N. Rao (Academic, New York, 1977), Vol. 2, p. 127.
[11] J. M. Brown and F. Jorgenson, Adv. Chem. Phys. **52**, 117 (1983).
[12] J. M. Brown, in *Computational Molecular Spectroscopy*, edited by P. Jensen and P. R. Bunker (Wiley, New York, 2000), p. 517.
[13] S. Carter and N. C. Handy, Mol. Phys. **47**, 1445 (1982); **52**, 1367 (1984).
[14] R. Barrow, R. N. Dixon, and G. Duxbury, Mol. Phys. **27**, 1217 (1974); A. Alijah and G. Duxbury, *ibid.* **70**, 605 (1990); G. Duxbury, B. McDonald, M. Van Gogh, A. Alijah, Ch. Jungen, and H. Palivan, J. Chem. Phys. **108**, 2336 (1998).
[15] M. Peric, R. J. Buenker, and S. Peyerimhoff, Mol. Phys. **59**, 1283 (1986); M. Peric, S. Peyerimhoff, and R. J. Buenker, Z. Phys. D: At., Mol. Clusters **24**, 177 (1992).
[16] P. R. Bunker and P. Jensen, J. Mol. Spectrosc. **118**, 18 (1986); *Molecular Symmetry and Spectroscopy* (NRC Research, Ottawa, 1998).
[17] M. Peric, S. Jerosimic, R. Rankovic, M. Krmar, and J. Radic-Peric, Chem. Phys. **330**, 60 (2006);
[18] M. Baer and A. Alijah, Chem. Phys. Lett. **319**, 489 (2000); M. Baer, S. H. Lin, A. Alijah, S. Adhikari, and G. D. Billing, Phys. Rev. A **62**, 032506 (2000); M. Baer, *Beyond Born Oppenheimer; Electronic Non-Adiabatic Coupling Terms and Conical Intersections* (Ref. 3), Chap. 2.
[19] H. A. Jahn and E. Teller, Proc. R. Soc. London, Ser. A **161**, 220 (1937).
[20] M. S. Child and H. C. Longuet-Higgins, Philos. Trans. R. Soc. London, Ser. A **254**, 259 (1961); G. Herzberg and H. C. Longuet-Higgins, Discuss. Faraday Soc. **35**, 77 (1963); H. C. Longuet-Higgins, Proc. R. Soc. London, Ser. A **344**, 147 (1975).
[21] E. R. Davidson, J. Am. Chem. Soc. **99**, 397 (1977).
[22] M. Baer and G. D. Billing, *The Role of Degenerate States in Chemistry*, Advances in Chemical Physics Vol. 124 (Wiley-Interscience, New York, 2002); M. S. Child, *ibid.*, p. 1; S. Adhikari and G. D. Billing, *ibid.*, p. 143; R. Englman and A. Yahalom, *ibid.*, p. 197; A. Kuppermann and R. Abrol, *ibid.*, p. 323.
[23] M. Chajia and R. D. Levine, Phys. Chem. Chem. Phys. **1**, 1205 (1999); K. L. Kompa and R. D. Levine, Proc. Natl. Acad. Sci. U.S.A. **98**, 410 (2001).
[24] M. Baer and R. Englman, Mol. Phys. **75**, 283 (1992); Z.-R. Xu, M. Baer,

and A. J. C. Varandas, J. Chem. Phys. **112**, 2746 (2000); J. Avery, M. Baer, and G. D. Billing, Mol. Phys. **100**, 1011 (2002); G. D. Billing, M. Baer, and A. M. Mebel, Chem. Phys. Lett. **1**, 372 (2003).
[25] A. Kuppermann, in *Dynamics of Molecules and Chemical Reactions*, edited by R. E. Wyatt and J. Z. H. Zhang (Marcel, New York, 1996), p. 411; R. Abrol, A. Shaw, and A. Kuppermann, J. Chem. Phys. **116**, 1035 (2002).
[26] R. Baer, J. Chem. Phys. **117**, 7405 (2002); I. Ryb and R. Baer, *ibid.* **121**, 10370 (2004).
[27] (a) M. Baer, T. Vertsi, G. J. Halász, Á. Vibók, and S. Suhai, Faraday Discuss. **127**, 337 (2004); (b) A. M. Mebel, G. J. Halász, Á. Vibók, A. Alijah, and M. Baer, J. Chem. Phys. **117**, 991 (2002); (c) G. J. Halász, Á. Vibók, A. M. Mebel, and M. Baer, *ibid.* **118**, 3052 (2003); (d) Á. Vibók, G. J. Halász, S. Suhai, D. K. Hoffman, D. J. Kouri, and M. Baer, *ibid.* **33**, 024312 (2006).
[28] R. Englman and T. Vertesi, Phys. Lett. A **354**, 196 (2006); B. Sarkar and S. Adhikari, J. Chem. Phys. **124**, 074101-1 (2006); P. Puzari, B. Sarkar, and S. Adhikari, *ibid.* **121**, 707 (2004); E. S. Kryachko, Adv. Quantum Chem. **44**, 119 (2003); P. Barragan, L. F. Errea, A. Macias, L. Mendez, A. Riera, J. M. Lucas, and A. Aguilar, J. Chem. Phys. **121**, 11629 (2004); O. Godsi, C. R. Evenhuis, and M. Collins, *ibid.* **125**, 164321 (2006); S. Gomez-Carrasco, A. Aquado, M. Paniaqua, and O. Roncero, *ibid.* **125**, 104105 (2006); M. B. Sevryuk, L. Y. Rusin, S. Cavalli, and V. Aquilanti, J. Phys. Chem. A **108**, 8731 (2004).
[29] R. Englman, *The Jahn-Teller Effect in Molecules and Crystals* (Wiley Interscience, New York, 1972); I. B. Bersuker, Chem. Rev. (Washington, D.C.) **101**, 1067 (2001).
[30] M. Born and J. R. Oppenheimer, Ann. Phys. **84**, 457 (1927); M. Born, Festschrift Göttingen Nach. Math. Phys. **K1**, 1 (1951).
[31] M. Born and K. Huang, *Dynamical Theory of Crystal Lattices* (Oxford University, New York, 1954), Chap. 4.
[32] (a) M. Peric and S. D. Peyerimhoff, J. Chem. Phys. **102**, 3685 (1995); (b) M. Peric, B. Engels, and M. Hanrath, Chem. Phys. **238**, 33 (1998).
[33] (a) M. Baer, Chem. Phys. Lett. **35**, 112 (1975); (b) M. Baer, *Beyond Born Oppenheimer; Electronic Non-Adiabatic Coupling Terms and Conical Intersections* (Ref. 3), Chap. 2.
[34] (a) M. Baer, Mol. Phys. **40**, 1011 (1980); (b) M. Baer, *Beyond Born Oppenheimer; Electronic Non-Adiabatic Coupling Terms and Conical Intersections* (Ref. 3), Chap. 1.
[35] H.-J. Werner, P. J. Knowles, J. Almlöf *et al.*, MOLPRO is a package of *ab initio* programs.
[36] M. Baer, *Beyond Born Oppenheimer; Electronic Non-Adiabatic Coupling Terms and Conical Intersections* (Ref. 3), Sec. 5.1.